Acta Crystallographica Section F
Structural Biology and Crystallization Communications
ISSN 1744-3091

Expression, purification and crystallization of a novel nonstructural protein VP9 from white spot syndrome virus

Yang Liu, J. Sivaraman and Choy L. Hew*

Department of Biological Sciences, National University of Singapore, Singapore

Correspondence e-mail: dbshewcl@nus.edu.sg

Received 1 June 2006
Accepted 15 July 2006

The nonstructural protein VP9 from white spot syndrome virus (WSSV) has been identified and expressed in *Escherichia coli*. To facilitate purification, a cleavable His_6 tag was introduced at the N-terminus. The native protein was purified and crystallized by vapour diffusion against mother liquor containing 2 *M* sodium acetate, 100 m*M* MES pH 6.3, 25 m*M* cadmium sulfate and 3% glycerol. Crystals were obtained within 7 d and diffracted to 2.2 Å; they belonged to space group $P2_12_12_1$, with unit-cell parameters $a = 74.13$, $b = 78.21$, $c = 78.98$ Å and four molecules in the asymmetric unit. The selenomethionine-labelled protein produced isomorphous crystals that diffracted to approximately 3.3 Å.

1. Introduction

White spot syndrome virus (WSSV) is the major pathogen of penaeid shrimp, causing economic losses of huge proportions to the shrimp aquaculture industry worldwide. It has a wide host range, infecting several crustacean species including crab and crayfish. WSSV virions are ovoid to bacilliform in shape, with a tail-like appendage at one end. The virus contains a double-stranded DNA with an estimated size of 300 kbp (Yang *et al.*, 2001). Genetic analysis has indicated that WSSV is a representative of a new virus group known as *Nimaviridae* (Van Hulten *et al.*, 2001). In cultured shrimps, a cumulative mortality of up to 100% occurs within 10 d of infection, with no effective treatment available to date. To develop effective therapeutic agents, detailed structural and functional insights into the viral proteins are required. However, functional studies have been greatly hampered owing to the lack of a suitable cell line to act as the virus host. In the literature there are several reports of the identification and characterization of WSSV structural proteins, mainly by proteomics approaches (Huang *et al.*, 2002; Tsai *et al.*, 2004). To date, over 39 WSSV structural genes have been identified (Tsai *et al.*, 2004). Functional analyses of WSSV proteins remain challenging. Structure-based functional analysis is an important approach for elucidating the function of proteins. No such analysis has been reported for the WSSV proteins. In addition to the envelope and capsid proteins, nonstructural proteins are required for replication of the viral genome, production of the virus particle and inhibition of the host-cell functions. These proteins are therefore potential candidates for drug design and the development of vaccines. Here, we describe the crystallization of VP9, a novel non-structural protein from WSSV.

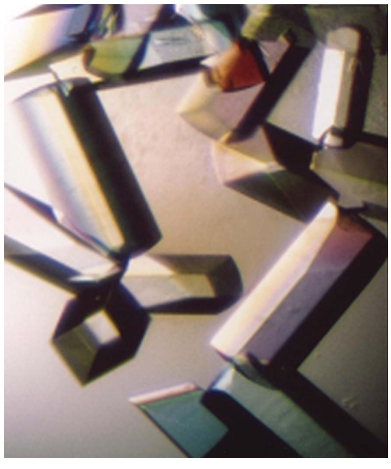

2. Cloning, expression and purification

Using specific primers 5′-CGCGCGCATATGGCCACCTTCCA-GACTGAC-3′ and 3′-CGCGGATCCTTATTCTGTTGTTGGCAC-5′, DNA coding for full-length (residues 1–82) VP9 was amplified by PCR from the purified WSSV virion. PCR products were further cloned into pET15b vector. The sequence was verified by DNA sequencing. The resulting construct was transformed into *Escherichia coli* strain BL-21 (DE3) for protein expression. Cells transformed with pET15b/nspVP9 were grown overnight at 310 K in 1 ml LB medium containing 100 µg ml^{-1} ampicillin. Cells were transferred into 1 l fresh LB medium and grown at 310 K. When the optical density at 600 nm (OD_{600}) reached about 0.8, 1 m*M* IPTG was added

to induce gene expression. The culture was grown for a further 4 h at 310 K. The cells were spun down at 6000 rev min^{-1} and resuspended in lysis buffer (20 m*M* Tris pH 8.0, 150 m*M* NaCl, 100 µ*M* PMSF). Cells were lysed by sonication followed by centrifugation at 18 000 rev min^{-1} at 277 K for 30 min. The supernatant was loaded onto an Ni^{2+}–NTA column; after substantial washing, the thrombin reaction was carried out on the resin to cleave the His tag. The eluted VP9 fractions from the Ni^{2+}–NTA column were passed through a Superdex-30 gel-filtration column using a buffer containing 20 m*M* Tris, 100 m*M* NaCl pH 8.0. Fractions were collected and concentrated to a final concentration of 20 mg ml^{-1} with an Amicon filter (Millipore, 10 000 Da molecular-weight cutoff) prior to crystallization. SeMet VP9 was produced using the same bacterial strain grown in M9 medium, to which 30 mg l^{-1} L-selenomethionine was added when the OD_{600} reached about 0.6–0.9 (Doublié & Carter, 1992). The SeMet VP9 was purified using the same protocol as the native VP9.

3. Characterization

The His-tag cleaved VP9 was 85 residues in length, which includes the full-length VP9 (82 amino acids) and three residues at the N-terminal (glycine, serine and histidine) from the thrombin cleavage site. Native and SDS polyacrylamide gel electrophoresis (SDS–PAGE) were performed to estimate the purities of VP9 (both native and SeMet) prior to crystallization. Fig. 1 shows the SDS–PAGE for native VP9 and SeMet. VP9 forms a dimer in solution as shown by gel filtration (Fig. 1*c*). The substitution of selenium was verified by MALDI–TOF mass spectrometry of SeMet-labelled and native VP9 (Fig. 2). The purified protein has been characterized further using dynamic light scattering (DLS) and circular dichroism (CD). The DLS experiments were conducted at different concentrations of the two proteins (1–5 mg ml^{-1}) which are threefold to fourfold lower than the initial protein concentrations used during crystallization. Both native and SeMet VP9 exist as dimers at all concentrations tested. CD spectra taken at 293–298 K show that both native and SeMet forms of VP9 contain highly similar secondary-structure contents (α-helices and β-strands; data not shown).

4. Crystallization

Purified native VP9 was concentrated to approximately 20 mg ml^{-1} in a buffer consisting of 20 m*M* Tris pH 8.0, 100 m*M* NaCl. The protein was crystallized by the hanging-drop vapour-diffusion method at 298 K. Initial crystallization screening was performed using the

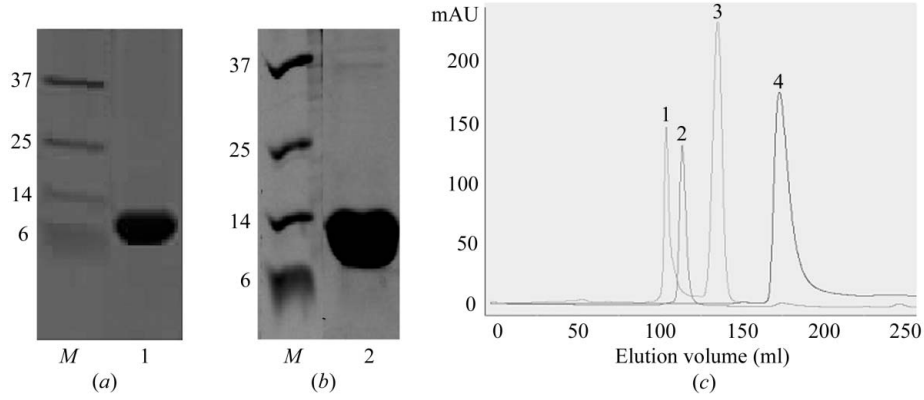

Figure 1
The purity of VP9 was characterized by 15% SDS–PAGE followed by Coomassie staining. Lane *M*, protein markers (kDa). (*a*) Lane 1, purified native VP9. (*b*) Lane 2, purified SeMet VP9. (*c*) The gel-filtration profile of VP9 together with marker proteins (1, thrombin, 37 kDa; 2, chymotrypsin, 25 kDa; 3, VP9 dimer, 18 kDa; 4, lysozyme, 14 kDa). This shows that VP9 eluted as a dimer.

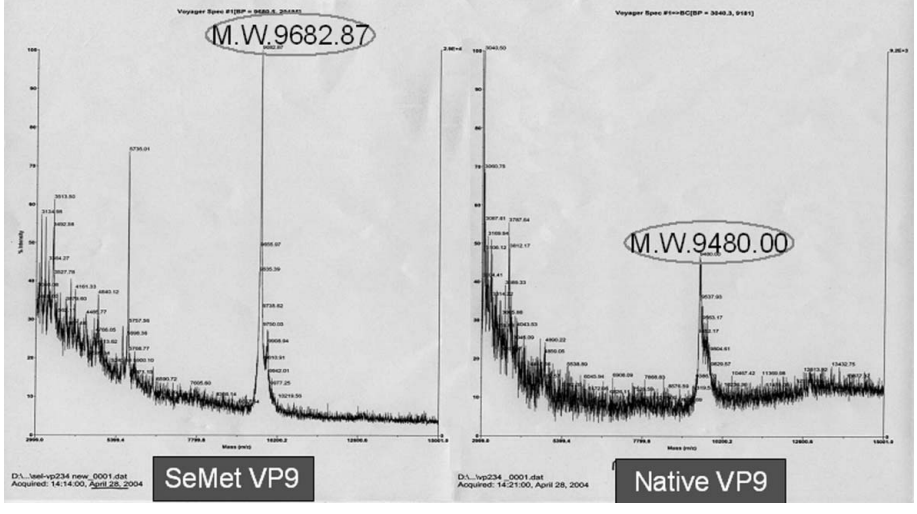

Figure 2
MALDI–TOF MS results for SeMet VP9 (left) and native VP9 (right). The mass spectra reveal a difference of approximately 200 Da, indicating the expected substitution of four Se atoms.

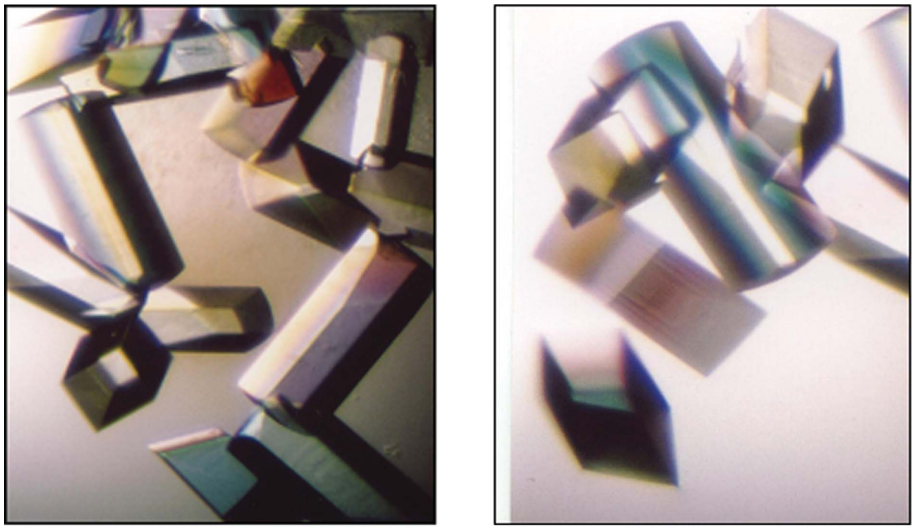

(*a*) (*b*)

Figure 3
Crystals of VP9. (*a*) Native. (*b*) SeMet.

Table 1
Data-collection statistics.

	SeMet (MAD)			
	Peak	Edge	High resolution	Sulfur SAD
Beamline (BNL)	X29-C	X29-C	X12-C	X12-C
Wavelength (Å)	0.9788	0.9792	1.1	1.70
Oscillation angle (°)	1	1	1	1
Space group	$P2_12_12_1$	$P2_12_12_1$	$P2_12_12_1$	$P2_12_12_1$
Unit-cell parameters				
a (Å)	78.33	78.84	74.13	73.33
b (Å)	83.64	83.67	78.21	76.97
c (Å)	90.48	90.52	78.98	78.37
Resolution limits (Å)	25–3.3	25–3.3	50–2.2	50–2.35
Observed *hkl*	83800	80964	249473	214496
Unique *hkl*	9341	9269	43491	21079
Redundancy	9.0	8.8	5.7	10.4
Completeness (%)	97.8	97.0	99.1	97.4
Overall $I/\sigma(I)$	10.4	10.1	15.6	15.0
R_{sym}† (%)	11.9	11.8	6.3	5.6

† $R_{sym} = \sum |I_i - \langle I \rangle| / \sum |I_i|$, where I_i is the intensity of the *i*th measurement and $\langle I \rangle$ is the mean intensity for that reflection.

sparse-matrix approach using kits from Hampton Research (Crystal Screens 1 and 2). During screening, 1 µl protein solution was mixed with 1 µl reservoir solution. The initial condition was further optimized and the best diffracting crystals were obtained with a reservoir solution consisting of 2 *M* sodium acetate, 100 m*M* MES pH 6.3, 25 m*M* cadmium sulfate and 3% glycerol. Crystals grew to approximate dimensions of ∼0.2 × 0.2 × 0.1 mm within 7 d (Fig. 3). Both native and SeMet-substituted crystals grew under essentially the same conditions and both belonged to the same crystal form with similar unit-cell parameters.

5. Data collection

Prior to mounting, both native and SeMet crystals were briefly soaked for ∼10 s in a cryoprotectant solution consisting of a 50:50 mixture of mineral oil and paraffin oil, picked up in a nylon loop and flash-cooled at 100 K in a nitrogen-gas cold stream (Oxford Cryosystems, Oxford, England). Synchrotron data were collected at the X12C beamline, NSLS, Brookhaven National Laboratory. X-ray fluorescence spectra recorded for the crystals of SeMet VP9 near the Se absorption edge were analyzed with the program *CHOOCH* (Evans & Pettifer, 2001) to determine the correct energies for the measurement of anomalous and dispersive differences. A complete MAD data set was collected at two wavelengths (peak and edge) using a Quantum 4 CCD detector (Table 1). Diffraction data were processed using the program *HKL*2000 (Otwinowski & Minor, 1997). The data extend to a resolution of 3.3 Å. Initial attempts at phase calculation were not successful. Since the native crystals diffracted better than the SeMet-substituted crystals, we collected a complete sulfur SAD data set from the native crystals of VP9 to a resolution of 2.35 Å at a wavelength of 1.7 Å using a CCD detector with an oscillation of 1.0° (Table 1). Diffraction data were processed using the program *HKL*2000 (Otwinowski & Minor, 1997). Crystals belonged to space group $P2_12_12_1$, with unit-cell parameters a = 73.33, b = 76.97, c = 78.37 Å. A value of V_M of 2.9 Å^3 Da^{-1} was calculated according to Matthews (1968) assuming the presence of four molecules in the asymmetric unit. Based on this calculation, the solvent content was estimated to be around 57.5%. Subsequently, a high-resolution data set was collected to 2.2 Å (Table 1). Structure determination is in progress.

The authors would like to acknowledge X12C and X29C beamlines, Brookhaven National Laboratory, NSLS for data collection and to thank Dr Anand Saxena for help during data collection. We also thank Mr Shashikant Joshi for valuable discussions. We acknowledge the facilities provided by the Protein and Proteomic Center (PPC), Department of Biological Sciences, National University of Singapore. Finally, the authors are grateful for the funding support by MOE (Ministry of Education of Singapore) to CLH.

References

Doublié, S. & Carter, C. W. Jr (1992). In *Crystallization of Nucleic Acids and Proteins. A Practical Approach*, edited by A. Ducruix & R. Giegé. Oxford University Press.
Evans, G. & Pettifer, R. F. (2001). *J. Appl. Cryst.* **34**, 82–86.
Huang, C., Zhang, X., Lin, Q., Xu, X., Hu, Z. & Hew, C. L. (2002). *Mol. Cell. Proteomics*, **1**, 223–231.
Hulten, M. C. van, Witteveldt, J., Peters, S., Kloosterboer, N., Tarchini, R., Fiers, M., Sandbrink, H., Lankhorst, R. K. & Vlak, J. M. (2001). *Virology*, **286**, 7–22.
Matthews, B. W. (1968). *J. Mol. Biol.* **33**, 491–497.
Otwinowski, Z. & Minor, W. (1997). *Methods Enzymol.* **276**, 307–326.
Tsai, J. M., Wang, H. C., Leu, J. H., Hsiao, H. H., Wang, A. H., Kou, G. H. & Lo, C. F. (2004). *J. Virol.* **78**, 11360–11370.
Yang, F., He, J., Lin, X., Li, Q., Pan, D., Zhang, X. & Xu, X. (2001). *J. Virol.* **75**, 11811–11820.